

## CORRECTION

Correction: Redox regulation of the yeast voltage-gated  $\text{Ca}^{2+}$  channel homolog Cch1p by glutathionylation of specific cysteine residues (doi:10.1242/jcs.202853)

Avinash Chandel and Anand K. Bachhawat

There were errors in *J. Cell Sci.* (2017) **130**, jcs202853 (doi:10.1242/jcs.202853).

The wrong anti-His blots were used to prepare Fig. 5C and Fig. 7G. The corrected figure panels for tunicamycin-treated cells in Fig. 5C and TRX mutants in Fig. 7G are shown here. The anti-His blot for pH=8.5 cells in Fig. 5C was vertically compressed during figure preparation and therefore has also been updated. All analysis was carried out on the correct replicate blots and is not affected by these errors. The online and PDF versions of the article have been updated and the authors apologise to readers for the errors, which do not impact the conclusions of the paper.

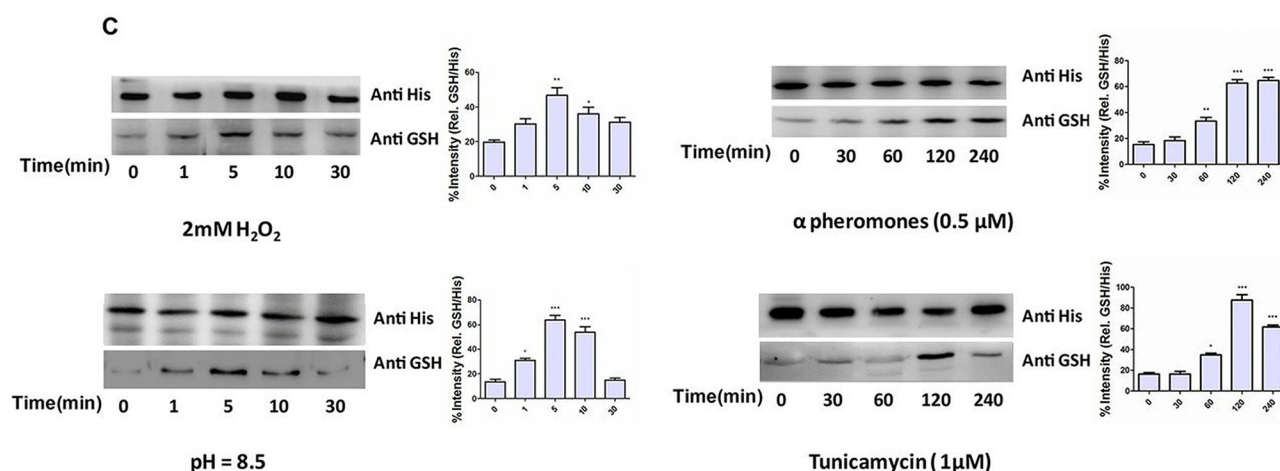


**Fig. 5C (corrected panel). Cch1p is glutathionylated under oxidative stress.** (C) Glutathionylation of Cch1p in response to fast and slow activation. WT cells overexpressing Cch1p with  $\text{OD}_{600\text{nm}}=1.5$  were treated with 2 mM  $\text{H}_2\text{O}_2$ , pH 8.5, 1  $\mu\text{M}$  tunicamycin or 0.5  $\mu\text{M}$   $\alpha$ -factor for different time intervals. The blots were probed with mouse anti-His and mouse anti-GSH primary antibodies and goat anti-mouse-IgG conjugated to HRP as secondary antibody. Densitometry results (graphs) represent the mean  $\pm$  s.d. of three independent biological replicates. \* $P < 0.05$ , \*\* $P < 0.01$ , \*\*\* $P < 0.001$ .

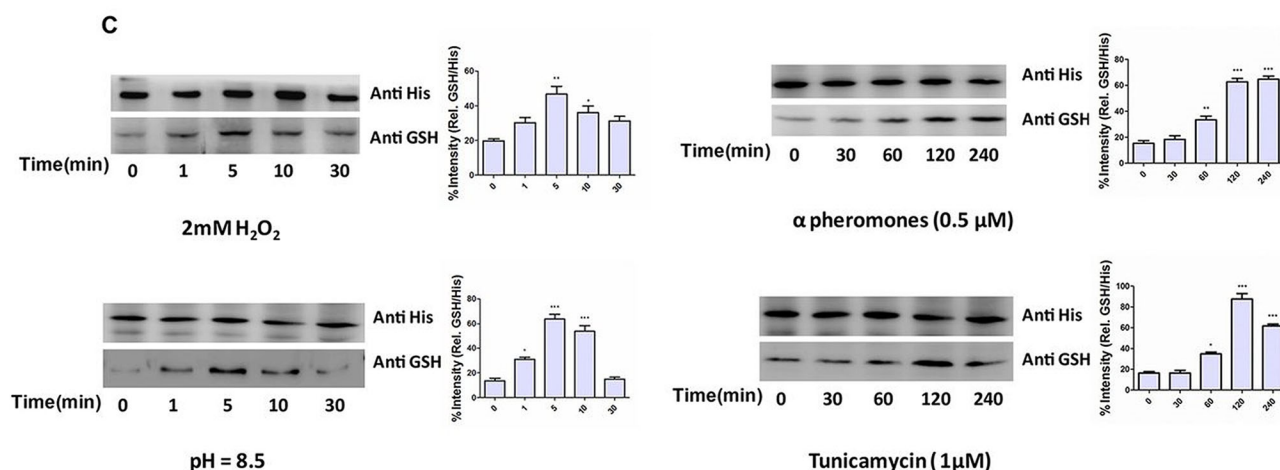


**Fig. 5C (original panel). Cch1p is glutathionylated under oxidative stress.** (C) Glutathionylation of Cch1p in response to fast and slow activation. WT cells overexpressing Cch1p with  $\text{OD}_{600\text{nm}}=1.5$  were treated with 2 mM  $\text{H}_2\text{O}_2$ , pH 8.5, 1  $\mu\text{M}$  tunicamycin or 0.5  $\mu\text{M}$   $\alpha$ -factor for different time intervals. The blots were probed with mouse anti-His and mouse anti-GSH primary antibodies and goat anti-mouse-IgG conjugated to HRP as secondary antibody. Densitometry results (graphs) represent the mean  $\pm$  s.d. of three independent biological replicates. \* $P < 0.05$ , \*\* $P < 0.01$ , \*\*\* $P < 0.001$ .

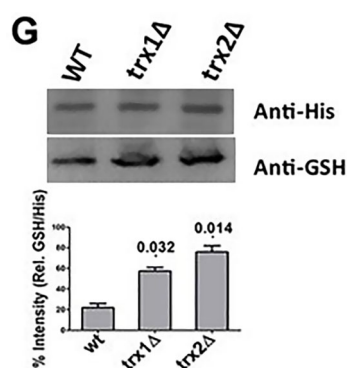


**Fig. 7G (corrected panel). Glutathionylation/deglutathionylation enzymes regulate Cch1 function.** (G) Glutathionylation analysis of Yvc1p in TRX mutants.

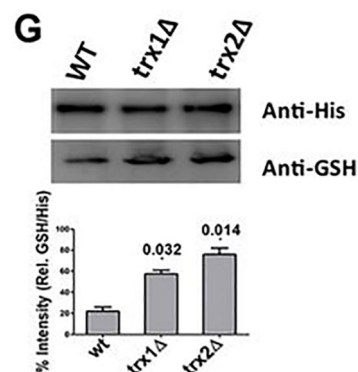


**Fig. 7G (original panel). Glutathionylation/deglutathionylation enzymes regulate Cch1 function.** (G) Glutathionylation analysis of Yvc1p in TRX mutants.

## RESEARCH ARTICLE

# Redox regulation of the yeast voltage-gated $\text{Ca}^{2+}$ channel homolog Cch1p by glutathionylation of specific cysteine residues

Avinash Chandel and Anand K. Bachhawat\*

## ABSTRACT

Cch1p, the yeast homolog of the pore-forming subunit  $\alpha_1$  of the mammalian voltage-gated  $\text{Ca}^{2+}$  channel (VGCC), is located on the plasma membrane and mediates the redox-dependent influx of  $\text{Ca}^{2+}$ . Cch1p is known to undergo both rapid activation (after oxidative stress and/or a change to high pH) and slow activation (after ER stress and mating pheromone activation), but the mechanism of activation is not known. We demonstrate here that both the fast activation (exposure to pH 8–8.5 or treatment with  $\text{H}_2\text{O}_2$ ) and the slow activation (treatment with tunicamycin or  $\alpha$ -factor) are mediated through a common redox-dependent mechanism. Furthermore, through mutational analysis of all 18 exposed cysteine residues in the Cch1p protein, we show that the four mutants C587A, C606A, C636A and C642A, which are clustered together in a common cytoplasmic loop region, were functionally defective for both fast and slow activations, and also showed reduced glutathionylation. These four cysteine residues are also conserved across phyla, suggesting a conserved mechanism of activation. Investigations into the enzymes involved in the activation reveal that the yeast glutathione S-transferase Gtt1p is involved in the glutathionylation of Cch1p, while the thioredoxin Trx2p plays a role in the Cch1p deglutathionylation.

**KEY WORDS:** Redox, Voltage-gated  $\text{Ca}^{2+}$  channels, Glutaredoxins, Glutathione S-transferase, Thioredoxins

## INTRODUCTION

Voltage-gated  $\text{Ca}^{2+}$  channels (VGCCs) on the plasma membrane of mammalian cells sense electrical potential changes across membranes and mediate the influx of  $\text{Ca}^{2+}$  into the cells (Catterall, 2000). VGCCs are composed of a large, pore-forming structural subunit  $\alpha_1$  and several auxiliary subunits, namely,  $\alpha_2$  or  $\delta$ ,  $\beta$  and  $\gamma$ , which regulate the function and efficient trafficking of the  $\alpha_1$  subunit to the membrane (Catterall et al., 2005; Jarvis and Zamponi, 2007).

In the yeast *Saccharomyces cerevisiae*, *CCH1* encodes a homolog of the pore-forming subunit  $\alpha_1$  of mammalian VGCCs. Like the mammalian voltage-gated  $\text{Ca}^{2+}$  channel  $\alpha_1$  subunit (known as CACNA1C), the Cch1p protein contains four structurally similar domains (I–IV), with each domain having six transmembrane domain (TMD) segments (Martin et al., 2011; Paidhungat and Garrett, 1997). To be functional, Cch1p needs another plasma membrane protein, Mid1p, which is broadly conserved in yeast and fungi and has been recently reported to resemble the mammalian  $\alpha$

and  $\delta$  subunit because of its structural features (Iida et al., 1994; Martin et al., 2011). Ecm7p, the third component of the Cch1p complex is related to the  $\gamma$  subunit of VGCCs and is a member of the claudin superfamily (Martin et al., 2011). Together, these three proteins form a high-affinity  $\text{Ca}^{2+}$  system (HACS) that can cause an influx of  $\text{Ca}^{2+}$  across the plasma membrane.

Although Cch1p shows significant sequence and structural homology to VGCCs,  $\text{Ca}^{2+}$  movement through Cch1p is not voltage dependent (Martin et al., 2011). Studies on Cch1p have revealed that it responds to different stimuli that include a sudden increase in pH (Viladevall et al., 2004), exposure to mating pheromones (Iida et al., 1994; Muller et al., 2001), store-operated stress (D'hooge et al., 2015; Locke et al., 2000), endoplasmic reticulum (ER) stress (Hong et al., 2010; Locke et al., 2000) and oxidative stress (Popa et al., 2010).

Cch1p-mediated  $\text{Ca}^{2+}$  influx activates the protein phosphatase calcineurin, which regulates the transcription of different target genes under certain stimuli (Bonilla et al., 2002). In a feedback mechanism, activated calcineurin has been reported to dephosphorylate Cch1p (Locke et al., 2000) and inhibit its activity. However, the presumed molecular mechanism of Cch1p regulation by kinases and phosphatases is not yet confirmed. The MAPK Slt2p is known to be required for Cch1p activation in response to tunicamycin, and the MAPK Fus3p is required for Cch1p activation in response to mating pheromones (Bonilla and Cunningham, 2003).

The redox state of the cell also controls ion channels/transporters, and these transporters can also reciprocally regulate the redox environment (Bogeski et al., 2010, 2011; Puigpinós et al., 2015). Thus, in higher organisms, different members of  $\text{Ca}^{2+}$ -conducting ion channels/transporters are known to be redox sensitive (Kozai et al., 2014; Todorovic and Jevtovic-Todorovic, 2014). In the yeast *Saccharomyces cerevisiae*, it has recently been shown that the yeast vacuolar  $\text{Ca}^{2+}$  channel Yvc1p, a member of the transient receptor potential (TRP) family of  $\text{Ca}^{2+}$  channels, responds to the redox state in the cell to regulate  $\text{Ca}^{2+}$  levels under conditions of glutathione depletion and extracellular oxidative stress through specific glutathionylation of cysteine residues (Chandel et al., 2016). As the yeast VGCC homolog, Cch1p also appears to respond to oxidative stress (Chandel et al., 2016; Popa et al., 2010), in the present study, we have investigated in detail the redox sensitivity of Cch1p. We show that Cch1p responds to the redox state in the cell and that both the rapid and the slow activation modes of Cch1p activation function in a conserved redox-dependent manner. We demonstrate that Cch1p is glutathionylated not only under oxidative stress but also under other channel-activating conditions. Mutational analysis confirmed that Cch1p glutathionylation occurs at specific cysteine residues, which results in channel activation and  $\text{Ca}^{2+}$  influx into the cytoplasm. Finally, we demonstrate that specific glutathionylation and deglutathionylation enzymes contribute to Cch1p regulation.

Department of Biological Sciences, Indian Institute of Science Education & Research (IISER), Sector 81, Mohali, Punjab 140306, India.

\*Author for correspondence (anand@iisermohali.ac.in)

 A.K.B., 0000-0003-1529-3769

Received 20 February 2017; Accepted 26 May 2017

## RESULTS

### Cch1p activation under oxidative stress

Previous studies have indicated that both Cch1p and Yvc1p respond to oxidative stress (Popa et al., 2010). To determine whether the responses of Cch1p and Yvc1p to oxidative stress followed similar patterns, we investigated the influx of  $\text{Ca}^{2+}$  into the cytoplasm during activation using individual deletions of these transporters, thereby ensuring that any interference could be eliminated. The time-dependent increase in cellular  $\text{Ca}^{2+}$  levels was measured by using the luminescent  $\text{Ca}^{2+}$  reporter aequorin (Nakajima-Shimada et al., 1991). In the wild-type (WT) yeast, exposure to 2 mM  $\text{H}_2\text{O}_2$  produces two waves of  $\text{Ca}^{2+}$  flux in yeast cells. An initial burst of  $\text{Ca}^{2+}$ , which lasts from between 1 and 5 min, followed by a second gradual activation, which begins at ~20 min and lasts for 10 min before returning to basal levels (Fig. 1). When we carried out the experiment with the deletion strains, we observed that, in *cch1Δ* cells, the first short-lived peak showed a dramatic 5-fold reduction in intensity. In contrast, the *yvc1Δ* cells showed almost no alterations in the first short-lived peak. When we examined the second  $\text{Ca}^{2+}$  peak in the different backgrounds, we observed that in *cch1Δ* cells, there was only a marginal drop in the second peak while in the *yvc1Δ* cells the second peak appeared to be absent (Fig. 1). These results indicate that the channels might be activated differently.

### Conservation of cytoplasmic and pore region cysteine residues in Cch1p

The Yvc1p channel has been investigated recently (Chandel et al., 2016), but considering the differences in the response profiles it was of great interest to understand the nature of the Cch1p activation. The rapid Cch1p activation suggested that this protein may be regulated by post-translational mechanisms. As cysteine residues are important targets of the redox regulation, we carried out a detailed analysis of the cysteine residues in Cch1p (their locations and conservation patterns), prior to targeting them for mutational analysis. The Cch1p transporter is a protein of 2039 amino acids that has been predicted to be a multiple membrane-spanning transmembrane protein (Paidhungat and Garrett, 1997; Teng et al., 2013). We reevaluated the topology prediction using Constrained Consensus TOPology metaserver (CCTOP) in combination with the topology information from PDBTM, TOPDB and TOPDOM databases. This reanalysis confirmed the

earlier predictions that CCH1 has 24 TMDs (Paidhungat and Garrett, 1997; Teng et al., 2013). Furthermore, Cch1p contains a total of 28 cysteine residues. Ten cysteine residues were predicted to be on the intracellular side, three in the extracellular region and five on the pore regions of the third and fourth segment of the channel. The 18 cysteine residues that were not buried in the TMDs appeared to be potential candidate residues responsible for the redox sensitivity of the channel.

To examine the conservation pattern of the cysteine residues we compared the amino acid sequences of the other members of the VGCC family. Fig. 2A shows a portion of multiple amino acid sequence alignment of the conserved cysteine residues in the seven species, including humans, yeast and representative model organisms such as mice, rat, zebrafish, fruit flies and nematodes. This alignment clearly indicates that the four cysteine residues in an internal loop connecting TMD4 and TMD5 of segment I and two residues at each pore region of segment III and segment IV were completely conserved across the species from yeast to humans (Fig. 2A). This remarkable conservation of the cysteine residues suggested that they could either have a critical structural role or could play a role in redox regulation of Cch1p, as well as other members of the VGCC family. However, while investigating the importance of the conserved cysteine residues, we decided to take a more unbiased approach and therefore included other exposed cysteine residues in the mutational analysis to see whether they might have a role in the redox regulation.

### Mutants of conserved cysteine residues show partial loss of function

The role of cysteine residues in redox sensitivity of Cch1p was examined by mutating all the 18 exposed cysteine residues including the eight conserved cysteine residues. The conserved cysteine residues were C587, C606, C636, C642, C1369, C1379, C1727 and C1738. The other exposed cysteine residues were C690, C696, C798, C1169, C1318, C1581, C1707, C1894, C1915 and C1955 and were also included in the study. Owing to the toxicity of this gene product in *E. coli*, the cloning was carried out in yeast using the previously defined homologous recombination strategy (Iida et al., 2004; Vu et al., 2009) as described in the Materials and Methods. The WT and mutants were functionally assayed by determining the oxidative stress ( $\text{H}_2\text{O}_2$ ) sensitivity. The results show that, compared to control Cch1p, which shows sensitivity to oxidative stress, six cysteine mutants showed a partial loss of function (i.e. rescue of cell death at 2.2 mM  $\text{H}_2\text{O}_2$ ) (Fig. 2B). Interestingly, all these six cysteine residues (C587, C606, C636, C642, C1369 and C1727) were from among the eight conserved cysteine residues. These included the four intracellular loop cysteine residues (C587, C606, C636, C642) and one from each of the pore regions (C1369 and C1727). All the other cysteine to alanine mutants appeared to be functional as they showed the same phenotype on the plate as control Cch1p. The functionality of all the cysteine to alanine mutants was also checked by exposure to the ER stress-inducing agent tunicamycin, which is a treatment that requires a functional Cch1p for cell survival (Fig. S1).

The loss of function seen in the cysteine mutants could be due to loss of channel function, a defect in localization to the plasma membrane or due to decreased expression of the mutant protein. To address these possibilities, we first checked the expression of the six defective cysteine mutants (C587A, C606A, C636A, C642A, C1369A and C1727A) by western blotting and found that there was no significant difference in the expression levels of the mutants as compared to control Cch1p (Fig. S2). We then checked the

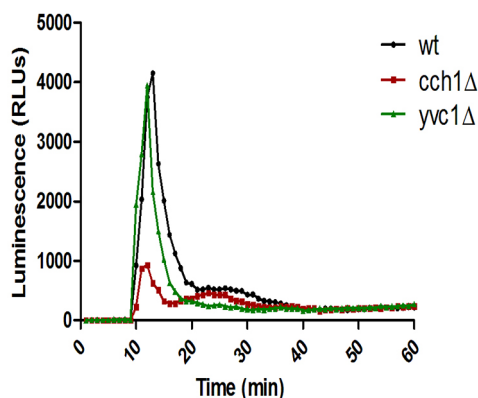


**Fig. 1. Cch1p activation takes place under oxidative stress.** Relative cytosolic  $\text{Ca}^{2+}$  levels represented as relative luminescence units over time in WT, *cch1Δ* and *yvc1Δ* cells. Each determination was repeated three times as independent experiments. The maximum RLU value obtained every second for each strain (obtained upon final detergent permeabilization and 10 mM  $\text{CaCl}_2$  treatment) was taken and graphs were plotted after normalization.



**A**

Species	Sequence	Length aa
H. sapiens Ca <sub>v</sub> 1.2(α <sub>1c</sub> )	295 HKTCTYNQEGI----ADVPAEDDPSPCAL 318	322-----G-HGRQC-QNGT-----VCKPGWDGP 339
M. musculus Ca <sub>v</sub> 1.2(α <sub>1c</sub> )	325 HKTCTYNQEGI----IDVPAEEDPSPCAL 348	351-----G-HGRQC-QNGT-----VCKPGWDGP 369
R. norvegicus Ca <sub>v</sub> 1.2(α <sub>1c</sub> )	325 HKTCTYNQEGI----IDVPAEEDPSPCAL 348	351-----G-HGRQC-QNGT-----VCKPGWDGP 369
D. rerio cacnalC	259 HASCYFGQTD-----ILEDEPAPCAV 279	281-----G-HGRTCPINGT-----LCKEGWQGP 300
D. melanogaster Ca_α1D	775 HKACRDEITG-----EYEENIRPCG- 794	795-----VGYYQCPPGY-----KCYGGWDGP 812
C. elegans egl5-19	248 HSTCIDPATG-----QLAQKDPTPCGT 269	672-----EGSAFKCQPSDSLTMGVRECSNNTTPWGP 302
S. cerevisiae Cch1	584 RRQCVWFNPEDPTD---TYQYDMQFCGG 608	627-----E-GSVSKGFLCPQYS-----KCVSNA-NP 648

\*                  \*                  \*                  \*

587                  606                  636                  642

H. sapiens Ca <sub>v</sub> 1.2(α <sub>1c</sub> )	1051 FKGLKLYTCSDSSK--QTAEACKGNITY 1077	1429 KKCAPESE-PSNSTEGETPCGS-SFAVFYFISFYMLCAFLII 1468.... 2138
M. musculus Ca <sub>v</sub> 1.2(α <sub>1c</sub> )	1081 FKGLKLYTCSDSSK--QTAEACKGNITY 1106	1459 KKCAPESE-PSNSTEGETPCGS-SFAVFYFISFYMLCAFLII 1498.... 2169
R. norvegicus Ca <sub>v</sub> 1.2(α <sub>1c</sub> )	1081 FKGLKLYTCSDSSK--QTAEACKGNITY 1106	1459 KKCAPESE-PSNSTEGETPCGS-SFAVFYFISFYMLCAFLII 1498.... 2170
D. rerio cacnalC	980 FKGFYRCNDEAK--SSPEECKGYIYL 1005	1347 KLCDPESD-YN--PGEEMTCGS-SFAIIYFTITFYMLCAFLII 1384.... 2168
D. melanogaster Ca_α1D	1495 FKGFKKCTDGSK--MTQDECYGTILVY 1521	1884 VKCDMNSDTP-----GEPCCGS-STAYPYFISFYVLCSFLII 1918.... 2516
C. elegans egl5-19	949 FGKTFFLCNLSK--MTAEACRGEYIH 974	1317 VRCDPMDDYHKGGLNESRCGN-NFAYPYFISFFMLCSFLVI 1357.... 1877
S. cerevisiae Cch1	1362 FKGLRGTCNDGSL---GRADCYNEYSNS 1386	1725 PYCSSDDN-----STYTDGSETYAYLLMSWNIIISMIFV 1760.... 2039

\*\*\* : \* \*                  \* \* :                  \*                  \*\*                  \*                  :: : : : : :

1369                  1379                  1727                  1738

**B**

NH2

Cytoplasm

COOH

**C**

No. of cells	cch1Δ	CCH1	C587A	C606A	C636A	C642A	C690A	C696A	C798A	C1169A	C1318A	C1369A	C1378A	C1581A	C1707A	C1727A	C1738A	C1894A	C1915A	C1955A
4 X 10 <sup>4</sup>	[Spot]	[Spot]	[Spot]	[Spot]	[Spot]	[Spot]	[Spot]	[Spot]	[Spot]	[Spot]	[Spot]	[Spot]	[Spot]	[Spot]	[Spot]	[Spot]	[Spot]	[Spot]	[Spot]	[Spot]
4 X 10 <sup>3</sup>	[Spot]	[Spot]	[Spot]	[Spot]	[Spot]	[Spot]	[Spot]	[Spot]	[Spot]	[Spot]	[Spot]	[Spot]	[Spot]	[Spot]	[Spot]	[Spot]	[Spot]	[Spot]	[Spot]	[Spot]
4 X 10 <sup>2</sup>	[Spot]	[Spot]	[Spot]	[Spot]	[Spot]	[Spot]	[Spot]	[Spot]	[Spot]	[Spot]	[Spot]	[Spot]	[Spot]	[Spot]	[Spot]	[Spot]	[Spot]	[Spot]	[Spot]	[Spot]
4 X 10 <sup>1</sup>	[Spot]	[Spot]	[Spot]	[Spot]	[Spot]	[Spot]	[Spot]	[Spot]	[Spot]	[Spot]	[Spot]	[Spot]	[Spot]	[Spot]	[Spot]	[Spot]	[Spot]	[Spot]	[Spot]	[Spot]

**Control**

[Spot]	[Spot]	[Spot]	[Spot]	[Spot]	[Spot]	[Spot]	[Spot]	[Spot]	[Spot]	[Spot]	[Spot]	[Spot]	[Spot]	[Spot]	[Spot]	[Spot]	[Spot]	[Spot]	[Spot]	[Spot]
--------	--------	--------	--------	--------	--------	--------	--------	--------	--------	--------	--------	--------	--------	--------	--------	--------	--------	--------	--------	--------

**H<sub>2</sub>O<sub>2</sub> 2.2mM**

proteins show proper colocalization with Pma1p. Taken together, we conclude that all the six functionally defective cysteine mutations result in loss of channel function of Cch1p and not in expression or membrane localization.

### Cch1p cysteine mutants show loss of fast and slow activation

Cch1p has been reported to undergo fast activation in response to high pH exposure (Viladevall et al., 2004) and oxidative stress. We also observed rapid transient activation of Cch1p in response to extracellular oxidative stress. In addition to the fast activation, a slower activation of Cch1p is observed during prolonged exposure to mating pheromones and ER stress-inducing agents (Bonilla and Cunningham, 2003; Zhang et al., 2006). To further explore the role of conserved cysteine residues in all these activation mechanisms, we exposed the Cch1p mutants to high pH,  $\alpha$ -factor pheromones and tunicamycin, and checked the growth phenotype. We observed that high pH-induced  $\text{Ca}^{2+}$  flux, which causes death in cells that express functional Cch1p, can be partially rescued in *CCH1* mutants showing loss of function under high pH stress (Fig. 3A). On the other hand, exposure to the  $\alpha$ -factor mating pheromone and tunicamycin, which are treatments that require functional Cch1p for cell survival, leads to significant loss of cell viability in *CCH1* mutants. This further confirms the non-functionality of *CCH1* mutants (Fig. 3A). To extend these growth-based results, we measured the  $\text{Ca}^{2+}$  levels in the cells up to a period of 4 h and found that the Cch1p cysteine to alanine mutants show partial loss of function in all the above conditions (Fig. 3B). These results indicate that, although being multimodal in nature, there is a unifying mechanism for Cch1p activation in the cell that responds to both fast as well as slow activation conditions.

### Cch1p activation responds to the redox state in the cell

The multiple effectors of Cch1p function that involve oxidative stress, high pH,  $\alpha$ -factor mating pheromone and tunicamycin were all unable to activate Cch1p when critical cysteine residues were mutated. Fast activation stress, like high pH, has been previously shown to result in oxidative stress in *Saccharomyces cerevisiae* (Viladevall et al., 2004). Slow activation mechanisms, like mating pheromone exposure, have also been shown to produce reactive oxygen species (ROS) in *S. cerevisiae* cells (Pozniakovsky et al., 2005; Zhang et al., 2006). Similarly, tunicamycin has also been shown to generate ROS in WT yeast cells (Rinnerthaler et al., 2012). Thus, it was of interest to determine whether an alteration in the redox environment of the cytosol might be causing these slow and fast activation effects, and the oxidizing state might be the common activation mechanism. We used the Grx1-roGFP<sub>2</sub> redox probe to measure the cytoplasmic redox state (Gutscher et al., 2008) in response to the fast activators of Cch1p ( $\text{H}_2\text{O}_2$  and pH 8) as well as the slow activators ( $\alpha$ -factor and tunicamycin). We observed a change in the redox state of the cells under all these conditions. However, with exposure to  $\alpha$ -factor pheromone and tunicamycin, this change was very slow, while it was very fast with  $\text{H}_2\text{O}_2$  and high pH stress (Fig. 4A). The change of redox correlated well with the time of the increase in cytoplasmic  $\text{Ca}^{2+}$ . This explains the slow activation of Cch1p upon exposure to these agents. The validity of the use of ro-GFP<sub>2</sub> probes at nonphysiological pH conditions has been contested, as the midpoint potential of ro-GFP<sub>2</sub> corresponds linearly to pH (Hanson et al., 2004). We therefore, used the ROS-sensitive fluorescent probe chloromethyl 2',7'-dichlorodihydrofluorescein diacetate probe (CM-H<sub>2</sub>DCFDA) to measure the cytoplasmic ROS levels in all our redox measurement experiments. We found a similar pattern in the ROS increase: rapid ROS generation after  $\text{H}_2\text{O}_2$  treatment and high pH stress and slow generation after  $\alpha$ -factor treatment and tunicamycin stress (Fig. 4B). These observations suggest that the redox sensitivity of Cch1p is a conserved mechanism of Cch1p activation.

### Cch1p is glutathionylated under conditions of both rapid activation and slow activation

The demonstration that specific cysteine residues are involved in the redox-dependent regulation of Cch1p suggested that post-translational modification is likely to be occurring at one or all of these residues. We initially examined whether disulfide bond formation might be occurring upon oxidative stress. We purified C-terminal His-tagged Cch1p from the cells exposed to 2 mM  $\text{H}_2\text{O}_2$  for 10 min and performed reducing versus non-reducing SDS gel analysis. No observable difference was observed in the mobility of reduced versus non-reduced His-tagged Cch1p (Fig. S3).

We subsequently examined whether glutathionylation of Cch1p might be occurring under  $\text{H}_2\text{O}_2$  stress, leading to the activation. We first carried out *in vitro* experiments to determine whether Cch1p can be glutathionylated. The glutathionylation was checked using an anti-GSH antibody which was verified for its specificity under reducing and non-reducing conditions (Fig. S4). The purified Cch1p protein was treated with 1 mM GSH and 400  $\mu\text{M}$  diamide. Glutathionylated Cch1p was detected by western blot analysis with anti-GSH antibody, and significant glutathionylation was observed. Blocking cysteine residues by pretreatment with alkylating agents like *N*-ethylmaleimide (NEM) and iodoacetamide (IAM) significantly reduced Cch1p glutathionylation (Fig. 5A). This confirms that specific glutathionylation of cysteine residues was occurring in Cch1p. To examine whether glutathionylation of Cch1p was also occurring *in vivo*, cells were exposed to diamide and  $\text{H}_2\text{O}_2$ . In both cases, a significant increase in the levels of Cch1p glutathionylation was observed (Fig. 5B).

We also examined whether Cch1p activation by  $\alpha$ -factor and tunicamycin might also be due to glutathionylation. Cells expressing Cch1p were exposed to 2 mM  $\text{H}_2\text{O}_2$ , pH 8.5, 400 nM tunicamycin and 0.5  $\mu\text{M}$   $\alpha$  pheromones for different time periods, spun down, washed and analyzed for glutathionylation as explained above. We observed an increase in glutathionylation levels of Cch1p (Fig. 5C). Although the increase is very prominent in the case of  $\text{H}_2\text{O}_2$  and high pH, in the case of tunicamycin and  $\alpha$ -factor pheromone, the increase is less prominent but is still significant. The protein levels, however, remain relatively unchanged in all the conditions. These results indicate the possible role of glutathionylation in activation of Cch1p.

### The cysteine to alanine mutants showing loss in function also show defective glutathionylation

A functional defect was observed in C587A, C606A, C636A, C642A, C1369A and C1727A mutants of Cch1p. This defect was observed in all the Cch1p-activating conditions. Since, thiol groups of the cysteine residues are involved in glutathionylation, we were interested to examine whether the loss of function correlated with the loss in glutathionylation. All the six mutant Cch1p proteins were purified from yeast cells exposed to oxidative stress ( $\text{H}_2\text{O}_2$ ) and examined for their glutathionylation. The mutants C1369A and C1727A, which were in the pore regions of segment III and IV showed no change in glutathionylation levels and were found to have similar glutathionylation levels to that of WT (Fig. 6). However, the mutants C587A, C606A, C636A and C642A, which were in the internal loop connecting TMD4 and TMD6 of segment I, had significantly lower levels of glutathionylation (Fig. 6). Pore region residues in ion channels have been associated with conformational changes of the channels (Hering et al., 2008), which decides the functionality of the channel. Thus, cysteine residues in the pore regions might not have any role in glutathionylation-mediated activation of Cch1p. On the other hand, the cytoplasmic cysteine

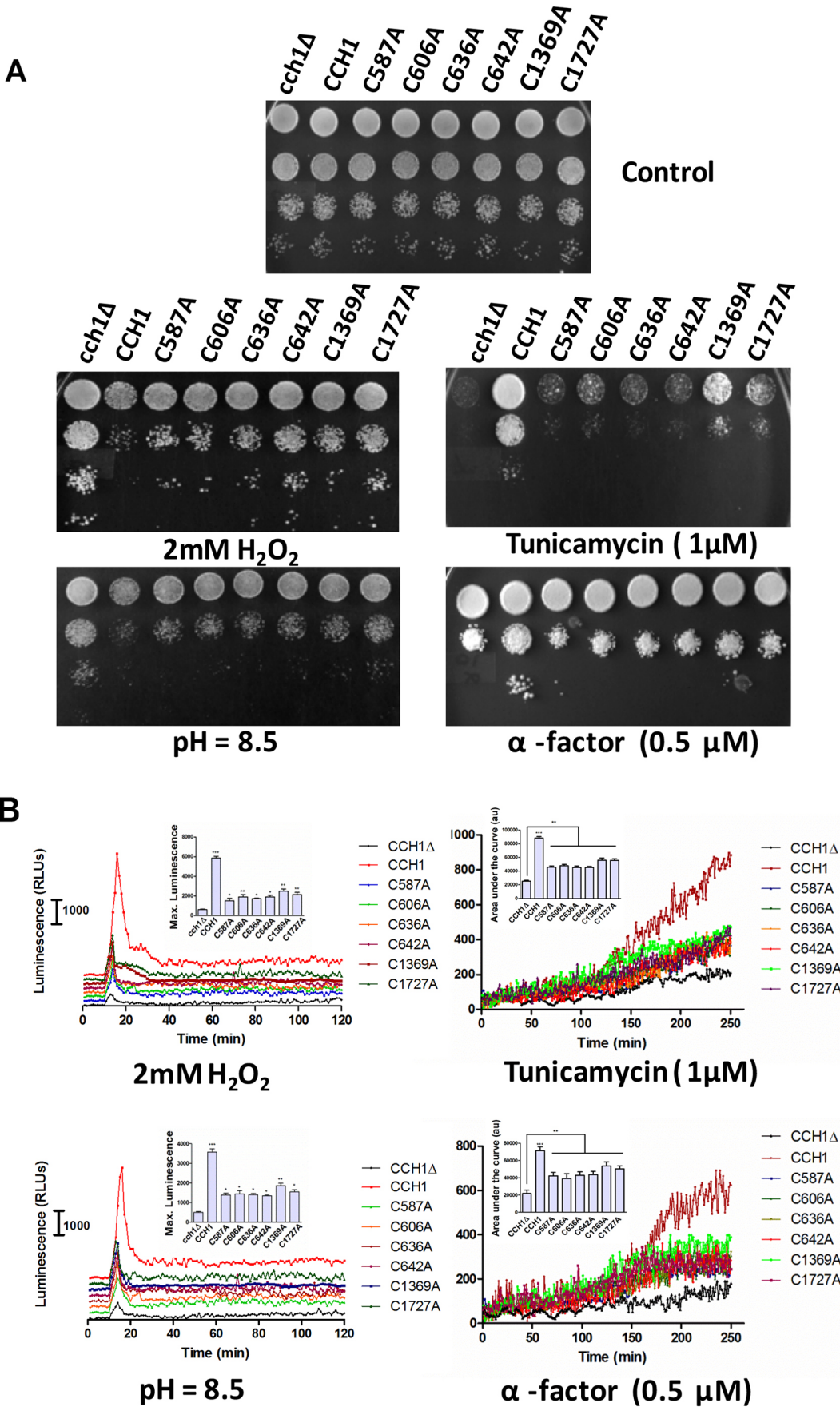


Fig. 3. See next page for legend.



**Fig. 3. Conserved Cch1p cysteine to alanine mutants show loss of fast and slow activation.** (A) Growth assay under different stress conditions.

Empty vector (pRS313TF), WT (CCH1) and all the six defective cysteine to alanine mutants were transformed into the *cch1Δ* strain. Transformants were grown to exponential phase in minimal medium, exposed to 2 mM H<sub>2</sub>O<sub>2</sub>, pH 8.5, 400 nM tunicamycin and 0.5 μM α-factor pheromone or not (control) and spotted onto minimal medium plates. The photographs were taken after 2–3 days of incubation at 30°C. (B) Ca<sup>2+</sup> influx under different stress conditions. Aequorin-based intracellular Ca<sup>2+</sup> measurement was performed by co-transforming the aequorin coding pEVP11/AEQ plasmid with empty vector (pRS313TF), WT CCH1 and all the six cysteine to alanine mutants in the *cch1Δ* strain. Exogenous stress of 2 mM H<sub>2</sub>O<sub>2</sub>, pH 8.5, 1 μM tunicamycin and 0.5 μM α mating pheromone was given after 10 min, and relative Ca<sup>2+</sup> levels were monitored up to 240 min. Each determination was repeated three times as independent experiments and mean of the three readings is plotted. The maximum luminescence intensity from three independent experiments was plotted as bar graphs [maximum RLU values for each strain (obtained upon final detergent permeabilization and 10 mM CaCl<sub>2</sub> treatment) were taken and graphs were plotted after normalization]. \**P*<0.05, \*\**P*<0.01, \*\*\**P*<0.001.

residues are always exposed to the intracellular redox conditions and accessible to modifications such as glutathionylation. These results correlated with the functional analysis and suggested that glutathionylation of these specific cysteine residues has a role in Cch1p regulation.

### Glutathionylation and deglutathionylation enzymes regulate Cch1 function

The observation that Cch1p glutathionylation at specific residues is essential for its activation suggested the possibility that enzymes that catalyze glutathionylation and deglutathionylation may also have a role in regulating Cch1p function. Glutathionylation of proteins has been shown to occur either enzymatically, or non-enzymatically (Mailloux et al., 2014) and glutathione S-transferases (belonging to the omega and pi family) are the main enzymes reported as being involved in glutathionylation in mammals (Manevich et al., 2004; Menon and Board, 2013).

We have recently shown that the unusual yeast glutathione S-transferase Gtt1p (which does not belong to any of the known classes) (Chandel et al., 2016) is involved in glutathionylation and activation of yeast vacuolar Ca<sup>2+</sup> channel Yvc1p. To examine whether Gtt1p or its homolog Gtt2p had a role in the activation of Cch1p, we examined the glutathionylation in *GTT1* and *GTT2* deletion backgrounds (*gtt1Δ* and *gtt2Δ*). The tagged *CCH1* gene was introduced into these different deletion backgrounds by the *in vivo* gap repair method as described in the Materials and Methods. Under oxidative stress, we observed a decrease in the Ca<sup>2+</sup> influx and a minor reduction in the glutathionylation of Cch1p in the case of *gtt1Δ* but not in the *gtt2Δ* background (Fig. 7A,B). This was also reflected in the growth, where *gtt1Δ* showed a slightly better growth as compared to WT backgrounds in these conditions (Fig. 7M). We then investigated these mutants upon activation with the slow activation agent α-factor pheromone. With exposure to α-factor, we also observed decreased glutathionylation in the case of *gtt1Δ* as compared to WT and *gtt2Δ* (Fig. 7C). We evaluated these mutants for Ca<sup>2+</sup> influx, and observed that the levels of intracellular Ca<sup>2+</sup> influx were lower in the *gtt1Δ* strain as compared to the WT in the case of α-factor stress (Fig. 7D). A growth assay also showed a defective growth for *gtt1Δ* upon α-factor exposure (Fig. 7O). These results clearly demonstrate a role for Gtt1p in the enzymatic glutathionylation of Cch1p during both the slow and fast activation mechanisms.

We also investigated the role for thioredoxins, glutaredoxins and sulfiredoxin as possible candidate enzymes involved in

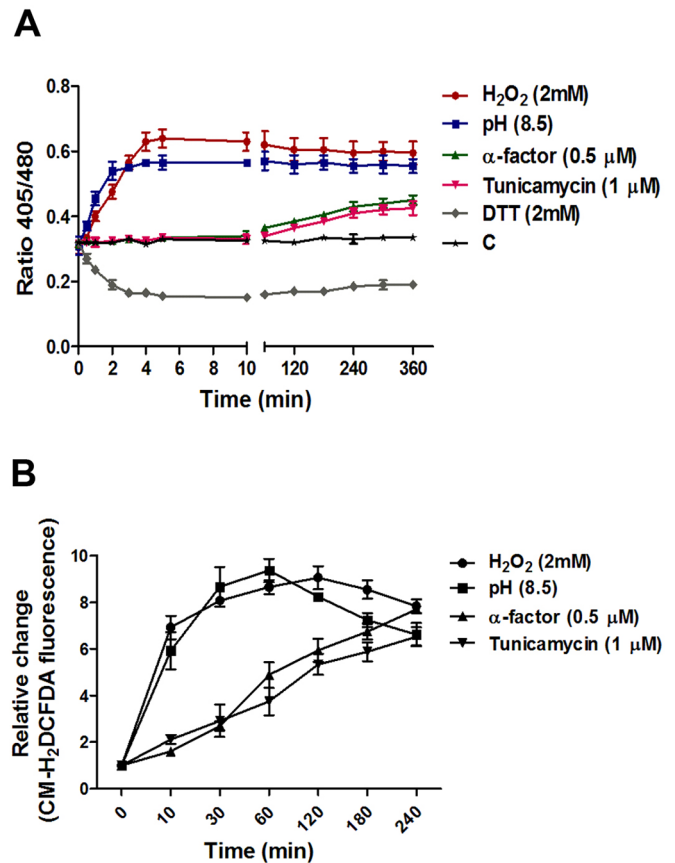


**Fig. 4. Effect of stress treatment on the redox state in the cell.**

(A) Measurement of glutathione redox state using Grx1-roGFP<sub>2</sub>. WT cells transformed with Grx1-roGFP<sub>2</sub> were exposed to 2 mM H<sub>2</sub>O<sub>2</sub>, pH 8.5, 400 nM tunicamycin or 0.5 μM α mating pheromone and the Grx1-roGFP<sub>2</sub> response was followed for 12 h. 2 mM H<sub>2</sub>O<sub>2</sub> and 5 mM DTT exposure were taken as a control for fully oxidized and fully reduced glutathione. The trace denoted C is a no-treatment control. The ratio of the fluorescence emission at 405 to 480 nm at fixed excitation of 510 nm is plotted against time. The graph shows the mean±s.d. ratio of the readings from three independent experiments. (B) Measurement of cytoplasmic ROS. Cells exposed to 2 mM H<sub>2</sub>O<sub>2</sub>, pH 8.5, 1 μM tunicamycin or 0.5 μM α-factor were harvested and suspended at OD<sub>600nm</sub>=0.1 in PBS containing 10 μM carboxymethyl-H<sub>2</sub>DCFDA and then analyzed by FACS. Results represent the mean±s.d. of *n*=3 independent biological replicates.

deglutathionylation since members of the thioredoxin fold family have been shown to have a role in deglutathionylation (Chandel et al., 2016; Findlay et al., 2006; Jung and Thomas, 1996). The His-tagged Cch1p protein was expressed in the different cytoplasmic glutaredoxin (*grx1Δ* and *grx2Δ*), thioredoxin (*trx1Δ* and *trx2Δ*) and sulfiredoxin (*srx1Δ*) mutant backgrounds and the glutathionylation status was examined. Among the different mutants, we observed that the *trx2Δ* (and to a lesser extent the *trx1Δ*) mutant showed increased glutathionylation (Fig. 7E,G). We evaluated these mutants for their ability to affect the Ca<sup>2+</sup> flux into the cell under conditions of Cch1p activation (oxidative stress or α-factor). We also observed here that the *trx2Δ* mutant (and to a lesser extent the *trx1Δ*) had high levels of Ca<sup>2+</sup> accumulation and the decay of Ca<sup>2+</sup> spike is delayed in them under fast activation i.e. oxidative stress (Fig. 7F,H). When we investigated the glutaredoxins, we observed that Cch1p glutathionylation levels were a little higher in *grx1Δ* cells (Fig. 7I), although the *P* value (0.057) was above the cut-off value of significance, and they also



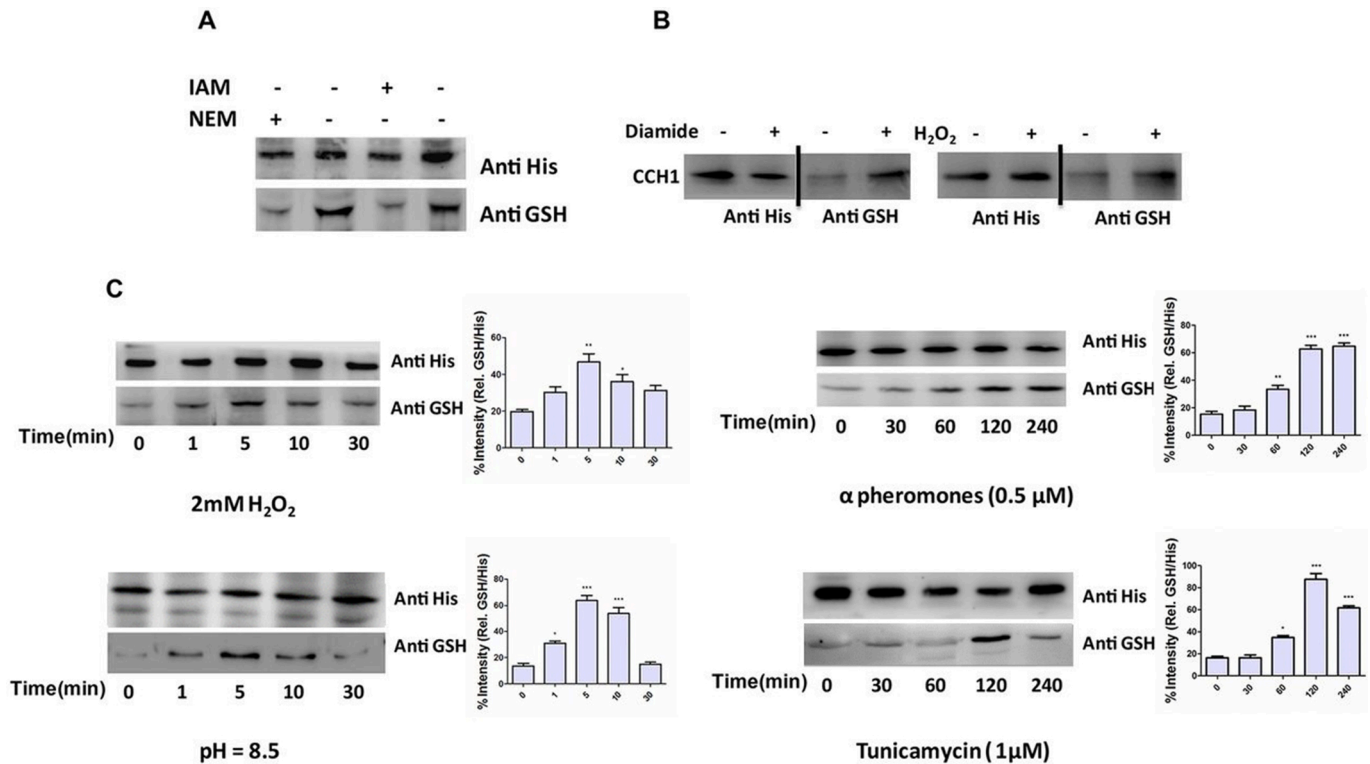


**Fig. 5. Cch1p is glutathionylated under oxidative stress.** (A) *In vitro* glutathionylation analysis of Cch1p. Purified Cch1p was incubated with GSH (1 mM) and diamide (400 μM) in the presence and absence of the cysteine-modifying agents N-ethylmaleimide (NEM) and Iodoacetamide (IAM) and analyzed by western blotting. (B) Diamide and H<sub>2</sub>O<sub>2</sub> increases glutathionylation of Cch1p *in vivo*. Cells overexpressing Cch1p with OD<sub>600nm</sub>=1.5 were treated with diamide (1 mM) and H<sub>2</sub>O<sub>2</sub> (1.5 mM) for 5 min. After washing, cells were lysed using glass beads and His-tagged Cch1p protein was purified using Ni-NTA beads and analyzed by western blotting. (C) Glutathionylation of Cch1p in response to fast and slow activation. WT cells overexpressing Cch1p with OD<sub>600nm</sub>=1.5 were treated with 2 mM H<sub>2</sub>O<sub>2</sub>, pH 8.5, 1 μM tunicamycin or 0.5 μM α-factor for different time intervals. After washing, cells were lysed using glass beads and His-tagged Yvc1p protein was purified using Ni-NTA beads and analyzed by western blotting. Western blotting analysis of above experiments was carried with an equal amount of protein resolved using 10% SDS-PAGE and electroblotted on nitrocellulose membrane. The blots were probed with mouse anti-His and mouse anti-GSH primary antibodies and goat anti-mouse-IgG conjugated to HRP as secondary antibody. Densitometry results (graphs) represent the mean±s.d. of three independent biological replicates. \**P*<0.05, \*\**P*<0.01, \*\*\**P*<0.001.

had higher Ca<sup>2+</sup> levels (Fig. 7J). Under slow activation conditions (α-factor), we also found a higher level of Ca<sup>2+</sup> in the *grx1Δ* mutant (Fig. 7L) and also an increased glutathionylation (Fig. 7K), although the *P* value (0.064) was above the cut-off value of significance. No change in the Cch1p glutathionylation was observed in thioredoxin and glutaredoxin mutants in the absence of stress (data not shown). To further show the effect of these responses on cell phenotype, we carried out growth viability assays for these strains on exposure to oxidative stress and α-factor. We found that both *grx1Δ* and *trx2Δ* showed sensitivity to oxidative stress (Fig. 7M), which has also already been reported (Collinson et al., 2002; Garrido and Grant, 2002; Luikenhuis et al., 1998) while on α-factor exposure, *grx1Δ* and *trx2Δ* strains showed significantly higher growth as compared to WT strain (Fig. 7O) (controls are shown in Fig. 7N). In addition to this, *cch1Δ* in *trx2Δ* and *grx1Δ* backgrounds partially rescues the sensitivity of *trx2Δ* and *grx1Δ* to oxidative stress (Fig. S5). These results indicate that Grx1p and Trx2p (and to a lesser extent, Trx1p) are involved in Cch1p deglutathionylation and its deactivation.

## DISCUSSION

In this work, we show how the yeast VGCC α<sub>1</sub> subunit homolog, Cch1p is regulated by redox through glutathionylation of specific cysteine residues (Fig. 8). Although there is strong evidence of redox regulation for different Ca<sup>2+</sup> channels (Popa et al., 2010;

Todorovic and Jevtovic-Todorovic, 2014), the mechanism of activation has not always been identified. In some cases, glutathionylation of these channels has also been demonstrated. In the VGCC channels, the cardiac VGCC L-type channel Ca<sub>v</sub>1.2 (known as CACNA1C) was found to be glutathionylated in ischemic human hearts (Johnstone and Hool, 2014; Tang et al., 2011). Purification of the protein from guinea pig heart also revealed that this protein was glutathionylated in response to oxidative stress, and the associated constitutive activity was thought to contribute to the pathology of the heart disease (Tang et al., 2011), but progress on characterizing the regulation of this class of transporters has been slow. One of the reasons for the relatively slow progress in studies on these channels has been the toxicity and instability of their cDNAs when expressed in *E. coli* (Clare, 2008). The yeast homolog is also toxic in *E. coli*, and thus in this work with Cch1p, the different mutants and constructs were created using the more arduous *in vivo* gap repair strategy which involves homologous recombination in yeast (Iida et al., 2004; Vu et al., 2009). This enabled a detailed alanine scanning of all the 18 exposed cysteine residues followed by functional analysis. An assessment of the glutathionylation status of the mutants revealed that four of the conserved cysteine residues (C587A, C606A, C636A and C642A) are responsible for the redox sensitivity and are targets for glutathionylation. Considering that the cysteine residues are conserved across phyla, one is tempted to suggest that this might

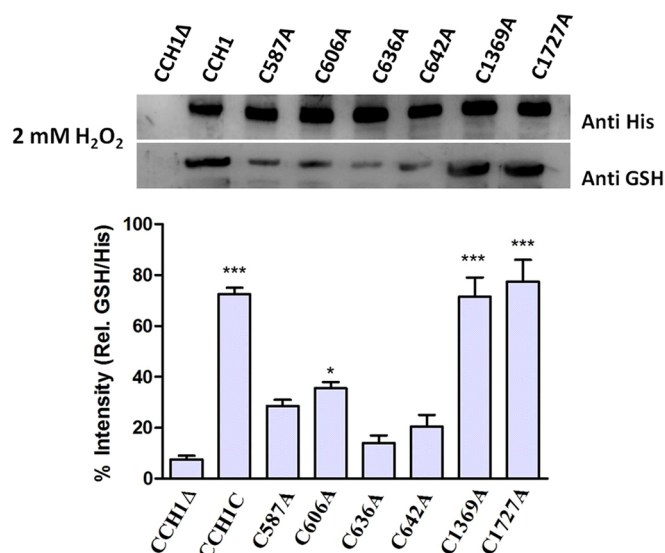


**Fig. 6. Specific cysteine residues are glutathionylated in Cch1p.**

Glutathionylation analysis of Cch1p mutants. Cch1p and mutant proteins were purified from a *cch1Δ* strain overexpressing WT (CCH1) and the defective cysteine mutants C587A, C606A, C636A, C642A, C1369A and C1727A after exposure to 2 mM  $H_2O_2$  for 5 min. Cells were harvested at  $OD_{600nm}=1.5$ . After washing, cells were lysed using glass beads and His-tagged protein was purified using Ni-NTA beads and analyzed by western blotting. Western blot analysis in the above experiments was carried with equal amounts of protein resolved using 10% SDS-PAGE and electroblotted on nitrocellulose membrane. The blots were probed with mouse anti-His and mouse anti-GSH primary antibodies and HRP-conjugated goat anti-mouse-IgG as secondary antibody. The total protein expression was then quantified by densitometry analysis of protein bands. The data are expressed as the percentage protein expression compared to control (anti-His) expression level and are the mean  $\pm$  s.d. of three independent experiments. \* $P<0.05$ , \*\*\* $P<0.001$ .

be a conserved mechanism of activation of all the proteins across phyla. In a recent study with the cardiac VGCC L-type channel, C543 was identified as a possible residue being involved in oxidative stress response although its role in glutathionylation was not determined (Muralidharan et al., 2016). This residue does not correspond to any of the CCH1 cysteine residues but is present in the internal loop critical for glutathionylation.

In addition to demonstrating the activation through glutathionylation during oxidative stress, we also observed that the sudden high pH exposure, another rapid activator of Cch1p-mediated  $Ca^{2+}$  influx (Martin et al., 2011), is also regulated through glutathionylation via the redox changes that are also observed to occur. Previously, this rapid activation has been presumed to act either through deprotonation of residues involved in ion conduction or alternatively through depolarization of the cell membrane (Chen et al., 1996; Martin et al., 2011). From studies described here, however, it is clear that there is an altered redox status that leads to glutathionylation and consequent activation of the channel. Interestingly, even the slow activation mechanism through ER stress (tunicamycin) or through mating pheromones ( $\alpha$ -factor) also seem to involve redox and glutathionylation. These latter pathways, although not fully understood, have been predicted to activate Cch1p through a calcineurin-dependent MAPK-dependent pathway (Bonilla and Cunningham, 2003; Muller et al., 2001). The current study reveals that Cch1p responds to both fast activation (high pH and  $H_2O_2$ ) and slow activation stress (tunicamycin and mating pheromones) in a similar manner that parallels the redox changes observed in the cell. Indeed, these various stress responses and

triggers in yeast cells have been reported to result in oxidative stress (Pozniakovskiy et al., 2005; Rinnerthaler et al., 2012; Viladevall et al., 2004; Zhang et al., 2006), underlining the possibility that activation of Cch1p is a conserved redox-dependent mechanism.

There are very few studies on the role of enzymes in specific glutathionylation events in yeasts. In the activation of Yvc1p, a role for the unusual glutathione S-transferase Gtt1p has been demonstrated (Chandel et al., 2016). Interestingly, we found here that Cch1p activation, which occurs much faster, is also dependent on Gtt1p. In fact, both the slow and fast activation of Cch1p was dependent on Gtt1p. Thus, not only is glutathionylation, the common activation mechanism for both slow or fast activation, but the enzymatic machinery also appears to be common for the two mechanisms. It will be of interest to see how the activity of Gtt1p itself is triggered.

When we examined the deglutathionylation of Cch1p, we observed that the thioredoxin Trx2p and glutaredoxin Grx1p were involved in the deglutathionylation process. This was observed both in the increased  $Ca^{2+}$  flux and the increased glutathionylation in these mutants. We observed that in both the slow and the fast activation, there was a common mechanism of deactivation. When we compare the activation of the two channels, it is interesting to note that the Trx2p protein can act on both Yvc1p and Cch1p, but Grx1p appeared to be unique in its action on Cch1p. Global glutathionylation patterns have interestingly revealed that *S. cerevisiae* mutants lacking Grx1p and Grx2p do not have high levels of protein glutathionylation, while a mutant lacking the cytosolic TRXs, Trx1p and Trx2p constitutively display protein hyperglutathionylation (Greetham et al., 2010). One possible explanation for the higher  $Ca^{2+}$  signals and increased glutathionylation in the *grx1Δ* strain is the high oxidizing conditions in the cells, since Grx1p has been shown to play a role in protection against oxidative stress (Izquierdo et al., 2010; Luikenhuis et al., 1998).

$Ca^{2+}$  flux into the cytoplasm of the yeast *S. cerevisiae* is tightly controlled by the opening and closing of two channels: the vacuolar channel Yvc1p and the plasma membrane channel whose principal subunit is Cch1p. We have previously shown that the activation of Yvc1p requires the specific glutathionylation that occurs during an altered redox state in the cell (Chandel et al., 2016). With this study, we show that the second major channel leading to the influx of  $Ca^{2+}$  into the cytosol, Cch1p, is also controlled by cytoplasmic redox state through specific glutathionylation of cysteine residues. Putting this together, it indicates that the redox status plays a major role in regulating the  $Ca^{2+}$  influx into the cytosol, even though the different channels access different  $Ca^{2+}$  stores. Further, these findings with the Cch1p, which corresponds to the  $\alpha$ -subunit of mammalian VGCC, should help to extend our understanding of structure–function relationship and regulation of VGCCs, a very important class of  $Ca^{2+}$  channels in living cells.

## MATERIALS AND METHODS

### Chemicals and reagents

All chemicals used in the present study were either of analytical or molecular biology grades and were obtained from commercial sources. Components for media were purchased from Difco. Oligonucleotides were purchased from Sigma and IDT. Restriction enzymes, Vent DNA polymerase and other DNA modifying enzymes were obtained from New England Biolabs. Gel extraction kits, plasmid miniprep columns and the Ni-NTA agarose resin were obtained from QIAGEN. Hybridization nitrocellulose membrane (filter type 0.45  $\mu m$ ) and Luminata™ forte western horseradish peroxidase (HRP) substrate was obtained from Millipore. Anti-His mouse monoclonal antibody (27E8; cat. no 2366) and horse anti-mouse-IgG HRP-linked antibody (cat. no. 7076) were procured

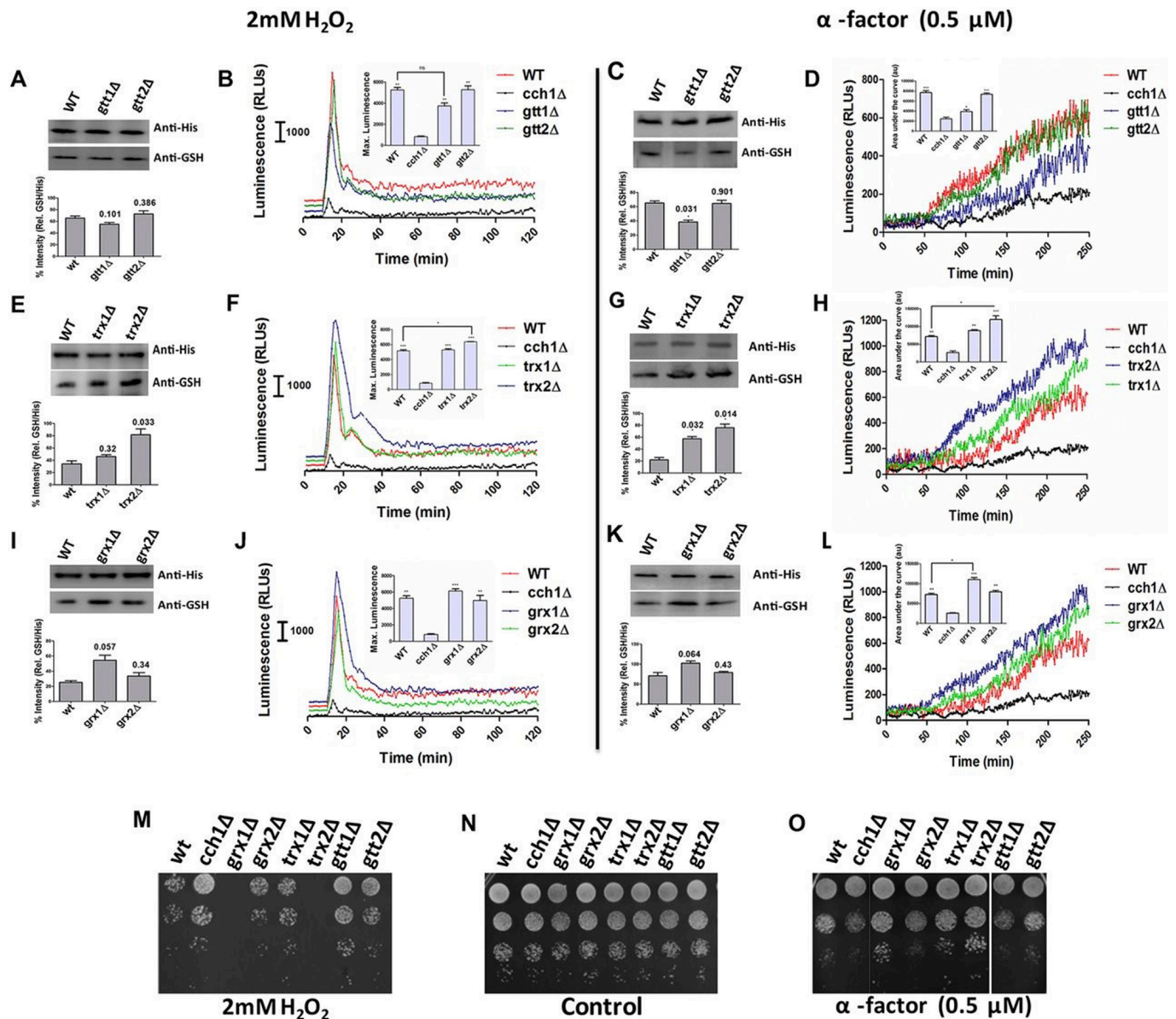


**Fig. 7. Glutathionylation/Deglutathionylation enzymes regulate Cch1 function.** Glutathionylation analysis of Yvc1p in GTT (A,C), TRX (E,G) and GRX (I,K) mutants. Cch1p protein was purified from WT (BY4741), *grx1Δ*, *grx2Δ*, *trx1Δ*, *trx2Δ*, *ggt1Δ* and *ggt2Δ* mutants after exposure to 2 mM  $H_2O_2$  or 0.5  $\mu M$   $\alpha$  mating pheromone. Cells were harvested at  $OD_{600nm}=1.5$ . After washing, cells were lysed using glass beads and His-tagged protein was purified using Ni-NTA beads and analyzed by western blotting. Western blot analysis was carried out with equal amounts of protein resolved using 10% SDS-PAGE and electroblotted on nitrocellulose membrane. The blots were probed with mouse anti-His and mouse anti-GSH primary antibodies and HRP-conjugated goat anti-mouse-IgG as secondary antibody. The total protein expression was then quantified by densitometry analysis of protein bands. The data are expressed as the percentage protein expression compared to control (anti-His) expression level, and are the mean  $\pm$  s.d. of three independent experiments. \* $P<0.05$ . A  $Ca^{2+}$  assay was also performed in the different GTTs (B,D), TRXs (F,H) and GRXs (J,L) mutant backgrounds. WT (BY4741), *cch1Δ*, *grx1Δ*, *grx2Δ*, *trx1Δ*, *trx2Δ*, *ggt1Δ* and *ggt2Δ* were transformed with *CCH1*, and aequorin-based intracellular  $Ca^{2+}$  measurement was done after exposure to 2 mM  $H_2O_2$  or 0.5  $\mu M$   $\alpha$  mating pheromone for 240 min. Maximum luminescence intensity (B,F,J) and the area under the curve (D,H,L) from three independent experiments was plotted as bar graphs. \* $P<0.05$ , \*\* $P<0.01$ , \*\*\* $P<0.001$ . Similarly, the maximum RLU value obtained every second for each strain (obtained upon final detergent permeabilization and 10 mM  $CaCl_2$  treatment) was taken and graphs were plotted after normalization. (M–O) Functional characterization of different enzyme mutants. WT, *cch1Δ* and all the enzyme mutants (*grx1Δ*, *grx2Δ*, *trx1Δ*, *trx2Δ*, *ggt1Δ* and *ggt2Δ*) were grown to exponential phase in minimal medium, exposed to (M) 2 mM  $H_2O_2$ , (N) no treatment (control) and (O) 0.5  $\mu M$   $\alpha$  mating pheromone and spotted on minimal medium plates. The photographs were taken after 2–3 days of incubation at 30°C.

from Cell Signaling Technology. Anti-GSH mouse monoclonal antibody D8 (ab19534) was from Abcam. Alexa Fluor 488-conjugated goat anti-mouse-IgG antibody was obtained from Molecular Probes. Coelenterazine was purchased from Promega.

#### Strains, plasmids and culture conditions

The strains used in this study are listed in Table S2. Plasmid pEVP11/AEQ (a plasmid bearing the apoaequorin gene and a LEU2 marker), was used for

$Ca^{2+}$  measurement experiments. pRS313TEF, a centromeric yeast vector with a HIS3 marker was used to clone and express *CCH1* and its mutants. The strains were maintained on yeast extract, peptone and dextrose (YPD) medium and grown at 30°C. The yeast transformants were selected and maintained on synthetic defined (SD) minimal medium containing yeast nitrogen base, ammonium sulfate and dextrose supplemented with the required amino acids. Yeast transformation was carried out by the lithium acetate method (Gietz et al., 1995).



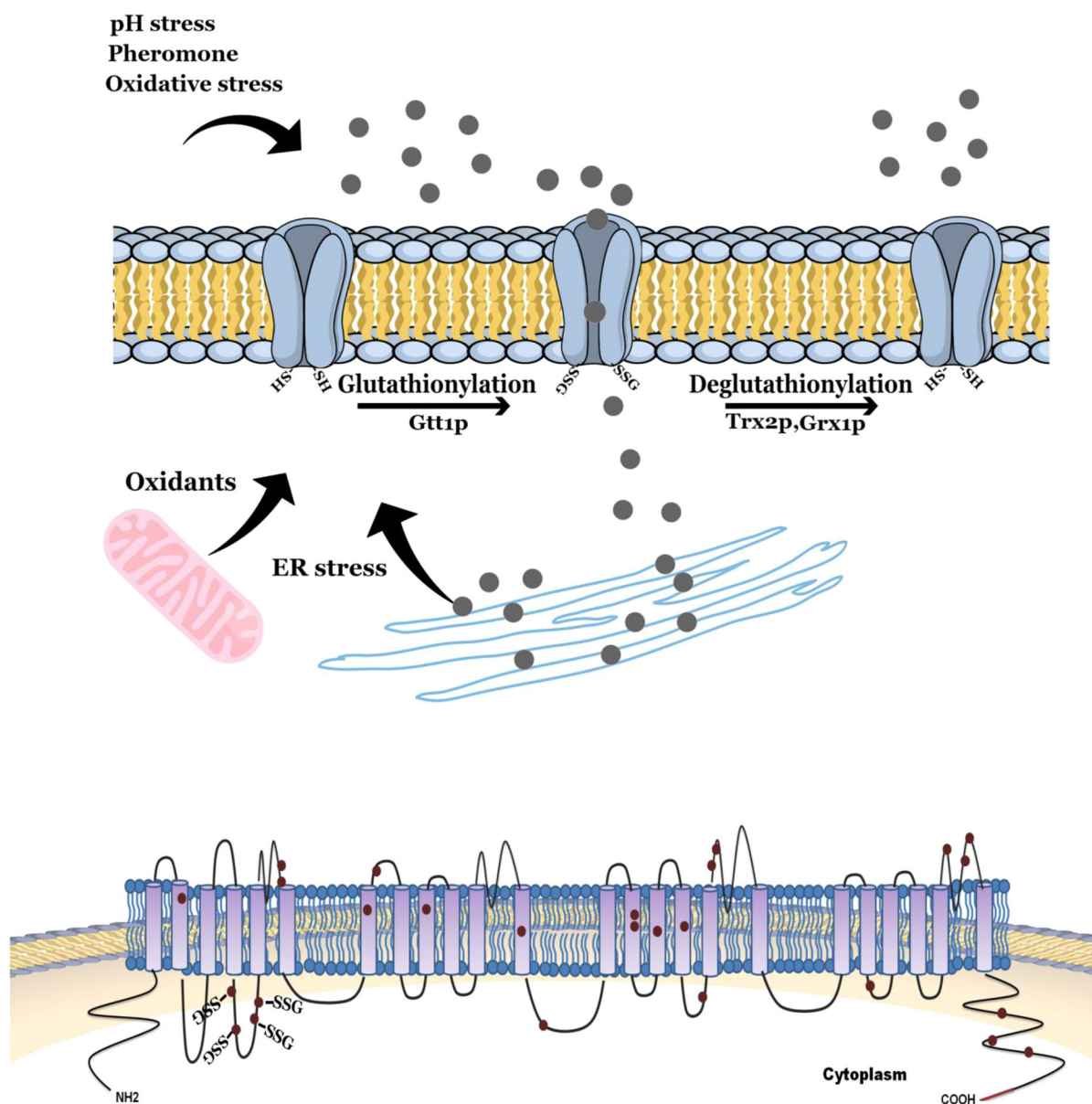


**Fig. 8. Model of the mechanism of Cch1p activation and restoration.** Cch1p is a structural subunit of plasma membrane  $\text{Ca}^{2+}$  influx channel. Multiple stress conditions that change the redox state of the cell towards a more-oxidizing state lead to an enzyme (Gtt1p)-dependent glutathionylation and activation of Cch1p. Furthermore, the removal of glutathione groups, i.e. deglutathionylation by enzymes Grx1p and Trx2p, can reverse this process resulting in the restoration of the resting state of the channel.

### Cloning of *CCH1* and cysteine mutants

Owing to the toxicity of *CCH1* in *Escherichia coli*, we used *in vivo* recombination as already described (Iida et al., 2004; Vu et al., 2009) with some modifications to clone *CCH1* and its cysteine mutants in yeast. Briefly, *CCH1* was amplified from *S. cerevisiae* chromosomal DNA using primers that possess a part of the *CCH1* non-coding region and vector sequence. The His<sub>6</sub> sequence was included in the reverse primer to His-tag the *CCH1* protein. Splice overlap extension strategy was used to mutate specific cysteine residues in *CCH1*. Primers used are mentioned in Table S1. The PCR products of WT *CCH1* and mutant *CCH1* was mixed with linearized pRS313TEF vector and transformed into the *cch1Δ* strain. The resulting transformants were selected on histidine selection plates and were further examined by sequencing of plasmids isolated from yeast transformants. The functionality of the gene was checked on tunicamycin plates, where deletion strains transformed with control vector shows loss of viability and WT *CCH1*-transformed yeast cells grow well.

### ROS estimation

ROS in yeast was quantified after growing cells in YPD medium at 30°C to late log phase after exposure to  $\alpha$ -factor, tunicamycin and different pH conditions for various times. Cells were then harvested, and  $10^4$  cells were stained with 10  $\mu\text{M}$  CM-H<sub>2</sub>DCFDA for 30 min at 30°C. The cells were then washed with 1× phosphate-buffered saline (PBS) and subjected to flow cytometric analysis at an excitation wavelength of 492 nm and emission of 520 nm using a BD Accuri flow cytometer.

### H<sub>2</sub>O<sub>2</sub>, pH, tunicamycin and $\alpha$ -factor sensitivity assay for Cch1p functionality

The yeast strains were transformed with plasmids containing either the WT *CCH1* or *CCH1* mutants. Transformants were selected and grown in SD minimal medium plus supplements without histidine. The primary overnight culture was used to re-inoculate the secondary culture and incubated until the optical density at 600 nm ( $\text{OD}_{600\text{nm}}$ ) = 0.6–1.5. Equal

numbers of cells were harvested, washed with water and suspended in fresh SD medium to  $OD_{600nm}=1$ . For  $H_2O_2$  stress experiments, cells were exposed to different concentrations ranging from 1 to 4  $\mu M$  of  $H_2O_2$  for 1 h. Cells were then washed, and serial dilutions were prepared, and 10  $\mu l$  of each dilution was spotted on to the SD medium. For pH exposure experiments, plates of different pH were made by making medium using Tris-HCl buffer instead of water, and pH was adjusted using 5 M NaOH. For  $\alpha$ -pheromone and tunicamycin exposure assays, different concentrations of these chemicals were added into the medium, and serial dilution of the cells were spotted. The plates were incubated at 30°C for 2–3 days, and then images were taken.

### Protein purification and western blot analysis

Cells exposed to extracellular agents  $H_2O_2$ , diamide, different pH, tunicamycin and  $\alpha$ -factor were harvested by centrifugation at 2500  $g$  for 5 min and washed subsequently with ice-cold water. The cell pellet was resuspended in 1 ml of homogenization buffer [50 mM Tris-HCl pH 7.4, 400 mM NaCl, 10% glycerol (v/v), 1% Triton-X, 1 mM PMSF and protease inhibitor mixture (Complete, EDTA-free; Roche)]. Glass beads (425–600  $\mu m$  diameter) were added, and cells were lysed in a bead-beater by vigorous mixing for a total of 10 min on ice (1 min  $\times$  10 mixing with a 1-min interval between shakings). Samples were centrifuged at 15,000  $g$  for 20 min, and the supernatant was incubated with 500  $\mu l$  Ni-NTA agarose (Qiagen) at 4°C for 2–3 h. Samples were cooled for 10 min on the ice before centrifugation at 100  $g$  for 1 min. Pellets were resuspended gently in 10 ml ice-cold wash buffer [50 mM Tris-HCl pH 7.4, 10% (v/v) glycerol, 300 mM NaCl, 30 mM imidazole pH 6.5, 1.5 mM PMSF] and the centrifugation was repeated. Two more washing steps were carried out with wash buffer. The slurry was resuspended in 200  $\mu l$  of elution buffer [50 mM Tris-HCl, pH 7.4, 10% (v/v) glycerol, 0.3 M Imidazole pH 6.5, 1.5 mM PMSF] and incubated at 4°C with gentle shaking for 5 min. Finally, slurry was centrifuged at 100  $g$  for 5 min, and the eluted protein supernatant was collected. Protein content was estimated by the Bradford method. Immunoblot analysis of Ni-NTA-purified WT Cch1p, and its mutants, was performed as follows. Equal amounts of protein samples denatured in 100 mM Tris-HCl, pH-8, 4% (w/v), 5 mM EDTA, 40% (v/v) glycerol and 0.05% (w/v) Bromophenol Blue at 40°C for 10 min were resolved by non-reducing SDS/PAGE (10% acrylamide gel), electroblotted onto nitrocellulose membrane and probed with mouse monoclonal anti-His and anti-GSH primary antibody at 1:3000. The proteins were finally probed with goat anti-mouse-IgG HRP-conjugated secondary IgG and visualized using chemiluminescence detection reagent. For *in vitro* glutathionylation, purified Cch1p was incubated with 1 mM GSH and 0.5 mM diamide. Purified protein was incubated with 10 mM IAM and NEM (1 h at pH 7.5) for cysteine alkylation. To quantify the protein expression levels, Image J software was used for the densitometry analysis of the band signals. The resulting signal intensity was normalized with respect to the band surface area and expressed as percentage expression levels compared to control Cch1p (anti-His antibody).

### Cellular localization of the Cch1p and cysteine mutants

To determine the localization of Yvc1p and its cysteine mutants, an indirect immunofluorescence protocol for budding yeast was followed (Kilmartin and Adams, 1984). Exponentially growing cultures were fixed for 2 h with 4% formaldehyde in 0.1 M potassium phosphate (pH 7.4). Cells were spheroplasted and permeabilized with 0.4% Triton-X before staining with rabbit monoclonal anti-His and mouse monoclonal antibody against the cell membrane marker protein Pma1p (Abcam ab113745, 1:3000). Primary antibody staining was detected with anti-rabbit-IgG conjugated to Alexa Fluor 647 and anti-mouse-IgG conjugated to Alexa Fluor 488 (Molecular Probes). Images were visualized for fluorescence and Nomarski optics using a Zeiss microscope with a 64 $\times$  oil objective and photographed using an AxioCam MRc5 camera.

### Determination of intracellular $Ca^{2+}$ levels

Cytosolic  $Ca^{2+}$  concentration was determined using the apoequorin expression system (Nakajima-Shimada et al., 1991). Yeast strains were transformed with the plasmid pEVP11/AEQ, containing the apoequorin

gene, and transformants were selected for growth on SD medium lacking leucine (SD-Leu). For luminescence assays, cells were grown overnight at 30°C in SD-Leu medium and harvested during exponential growth. These cells were resuspended at a density of about  $10^8$  cells/ml in fresh SD-Leu. To reconstitute functional aequorin, 5  $\mu M$  coelenterazine (stock solution 1 mM dissolved in methanol) was added and cells were incubated for 5 h at 30°C in the dark. Cells were collected by centrifuging at 2500  $g$  for 5 min, washed three times, resuspended in 200  $\mu l$  of medium and incubated for 30 min in order to reconstitute functional aequorin within the cells. After incubation, cells were transferred to a 96-well microplate. The baseline luminescence was recorded for 10 min and after addition of different chemicals the luminescence was recorded for 250 min. The light emission is reported as relative luminescence units (RLU) over time, for a similar number of cells per sample. Since light units cannot be accurately converted into intracellular  $Ca^{2+}$  concentrations, our results are presented as relative quantities. Cell lysis with 0.4% Triton-X plus 10 mM  $CaCl_2$  allowed confirmation that all measurements had been done in non-limiting conditions for aequorin. Multiple determinations were performed for each condition.

### Statistical analysis

In the western blot quantification, *P*-values were generated by ANOVA. Multiple comparisons were corrected by Bonferroni *t*-test (\**P*<0.05, \*\**P*<0.01, \*\*\**P*<0.001, *n*≥3 assays), respectively, in Prism 4 (GraphPad). All error bars represent mean±s.d. based on three independent experiments. In the fluorescence experiments, statistical analyses were performed using a paired Student's *t*-test.

### Acknowledgements

We thank Dr Patrick Masson, University of Wisconsin-Madison, USA for the pEVP11/AEQ plasmid.

### Competing interests

The authors declare no competing or financial interests.

### Author contributions

Conceptualization: A.C., A.B.; Methodology: A.C., A.B.; Software: A.C.; Validation: A.C.; Formal analysis: A.B.; Investigation: A.C., A.B.; Resources: A.B.; Data curation: A.C., A.B.; Writing - original draft: A.C.; Writing - review & editing: A.C., A.B.; Visualization: A.C., A.B.; Supervision: A.B.; Project administration: A.B.; Funding acquisition: A.B.

### Funding

The study was supported by a Grant-in-aid assistance (Project no. SB/SO/BB-017/2014) from the Department of Science and Technology, Ministry of Science and Technology, Government of India. A.C. is a recipient of a senior research fellowship from the Council of Scientific and Industrial Research, India. A.K.B. is a recipient of the JC Bose National Fellowship from the Department of Science and Technology, Ministry of Science and Technology, India.

### Supplementary information

Supplementary information available online at <http://jcs.biologists.org/lookup/doi/10.1242/jcs.202853.supplemental>

### References

- Bogeski, I., Kummerow, C., Al-Ansary, D., Schwarz, E. C., Koehler, R., Kozai, D., Takahashi, N., Peinelt, C., Griesemer, D. and Bozem, M. et al. (2010). Differential Redox Regulation of ORAI Ion Channels: A Mechanism to Tune Cellular Calcium Signaling. *Sci. Signal* **3**, ra24.
- Bogeski, I., Kappl, R., Kummerow, C., Gulaboski, R., Hoth, M. and Niemeyer, B. A. (2011). Redox regulation of calcium ion channels: chemical and physiological aspects. *Cell Calcium* **50**, 407–423.
- Bonilla, M. and Cunningham, K. W. (2003). Mitogen-activated protein kinase stimulation of  $Ca^{2+}$  signaling is required for survival of endoplasmic reticulum stress in yeast. *Mol. Biol. Cell* **14**, 4296–4305.
- Bonilla, M., Nastase, K. K. and Cunningham, K. W. (2002). Essential role of calcineurin in response to endoplasmic reticulum stress. *EMBO J.* **21**, 2343–2353.
- Catterall, W. A. (2000). From ionic currents to molecular mechanisms: the structure and function of voltage-gated sodium channels. *Neuron* **26**, 13–25.
- Catterall, W. A., Perez-Reyes, E., Snutch, T. P. and Striessnig, J. (2005). International Union of Pharmacology. XLVIII. Nomenclature and structure-function relationships of voltage-gated calcium channels. *Pharmacol. Rev.* **57**, 411–425.

- Chandel, A., Das, K. K. and Bachhawat, A. K. (2016). Glutathione depletion activates the yeast vacuolar transient receptor potential channel, Yvc1p, by reversible glutathionylation of specific cysteines. *Mol. Biol. Cell* **27**, 3913–3925.
- Chen, X. H., Bezprozvanny, I. and Tsien, R. W. (1996). Molecular basis of proton block of L-type  $\text{Ca}^{2+}$  channels. *J. Gen. Physiol.* **108**, 363–374.
- Clare, J. J. (2008). Functional expression of ion channels in mammalian systems. In *Protein Science Encyclopedia*, Wiley-VCH Verlag GmbH & Co. KGaA.
- Collinson, E. J., Wheeler, G. L., Garrido, E. O., Avery, A. M., Avery, S. V. and Grant, C. M. (2002). The yeast glutaredoxins are active as glutathione peroxidases. *J. Biol. Chem.* **277**, 16712–16717.
- D'hooge, P., Coun, C., Van Eyck, V., Faes, L., Ghillebert, R., Mariën, L., Winderickx, J. and Callewaert, G. (2015).  $\text{Ca}^{2+}$  homeostasis in the budding yeast *Saccharomyces cerevisiae*: impact of ER/Golgi  $\text{Ca}^{2+}$  storage. *Cell Calcium* **58**, 226–235.
- Findlay, V. J., Townsend, D. M., Morris, T. E., Fraser, J. P., He, L. and Tew, K. D. (2006). A novel role for human sulfiredoxin in the reversal of glutathionylation. *Cancer Res.* **66**, 6800–6806.
- Garrido, E. O. and Grant, C. M. (2002). Role of thioredoxins in the response of *Saccharomyces cerevisiae* to oxidative stress induced by hydroperoxides. *Mol. Microbiol.* **43**, 993–1003.
- Gietz, R. D., Schiestl, R. H., Willems, A. R. and Woods, R. A. (1995). Studies on the transformation of intact yeast cells by the LiAc/SS-DNA/PEG procedure. *Yeast* **11**, 355–360.
- Greetham, D., Vickerstaff, J., Shenton, D., Perrone, G. G., Dawes, I. W. and Grant, C. M. (2010). Thioredoxins function as deglutathionylase enzymes in the yeast *Saccharomyces cerevisiae*. *BMC Biochem.* **11**, 3.
- Gutscher, M., Pauleau, A.-L., Marty, L., Brach, T., Wabnitz, G. H., Samstag, Y., Meyer, A. J. and Dick, T. P. (2008). Real-time imaging of the intracellular glutathione redox potential. *Nat. Methods* **5**, 553–559.
- Hanson, G. T., Aggeler, R., Oglesbee, D., Cannon, M., Capaldi, R. A., Tsien, R. Y. and Remington, S. J. (2004). Investigating mitochondrial redox potential with redox-sensitive green fluorescent protein indicators. *J. Biol. Chem.* **279**, 13044–13053.
- Hering, S., Beyl, S., Stary, A., Kudrac, M., Hohaus, A., Guy, R. H. and Timin, E. (2008). Pore stability and gating in voltage-activated calcium channels. *Channels Austin Tex.* **2**, 61–69.
- Hong, M.-P., Vu, K., Bautos, J. and Gelli, A. (2010). Cch1 restores intracellular  $\text{Ca}^{2+}$  in fungal cells during endoplasmic reticulum stress. *J. Biol. Chem.* **285**, 10951–10958.
- Iida, H., Nakamura, H., Ono, T., Okumura, M. S. and Anraku, Y. (1994). MID1, a novel *Saccharomyces cerevisiae* gene encoding a plasma membrane protein, is required for  $\text{Ca}^{2+}$  influx and mating. *Mol. Cell. Biol.* **14**, 8259–8271.
- Iida, K., Tada, T. and Iida, H. (2004). Molecular cloning in yeast by in vivo homologous recombination of the yeast putative  $\alpha 1$  subunit of the voltage-gated calcium channel. *FEBS Lett.* **576**, 291–296.
- Izquierdo, A., Casas, C. and Herrero, E. (2010). Selenite-induced cell death in *Saccharomyces cerevisiae*: protective role of glutaredoxins. *Microbiol. Read. Engl.* **156**, 2608–2620.
- Jarvis, S. E. and Zamponi, G. W. (2007). Trafficking and regulation of neuronal voltage-gated calcium channels. *Curr. Opin. Cell Biol.* **19**, 474–482.
- Johnstone, V. P. A. and Hool, L. C. (2014). Glutathionylation of the L-type  $\text{Ca}^{2+}$  Channel in Oxidative Stress-Induced Pathology of the Heart. *Int. J. Mol. Sci.* **15**, 19203–19225.
- Jung, C.-H. and Thomas, J. A. (1996). S-glutathiolated hepatocyte proteins and insulin disulfides as substrates for reduction by glutaredoxin, thioredoxin, protein disulfide isomerase, and glutathione. *Arch. Biochem. Biophys.* **335**, 61–72.
- Kilmartin, J. V. and Adams, A. E. (1984). Structural rearrangements of tubulin and actin during the cell cycle of the yeast *Saccharomyces*. *J. Cell Biol.* **98**, 922–933.
- Kozai, D., Ogawa, N. and Mori, Y. (2014). Redox regulation of transient receptor potential channels. *Antioxid. Redox Signal.* **21**, 971–986.
- Locke, E. G., Bonilla, M., Liang, L., Takita, Y. and Cunningham, K. W. (2000). A homolog of voltage-gated  $\text{Ca}^{2+}$  channels stimulated by depletion of secretory  $\text{Ca}^{2+}$  in yeast. *Mol. Cell. Biol.* **20**, 6686–6694.
- Luikenhuis, S., Perrone, G., Dawes, I. W. and Grant, C. M. (1998). The yeast *Saccharomyces cerevisiae* contains two glutaredoxin genes that are required for protection against reactive oxygen species. *Mol. Biol. Cell* **9**, 1081–1091.
- Mailoux, R. J., Jin, X. and Willmore, W. G. (2014). Redox regulation of mitochondrial function with emphasis on cysteine oxidation reactions. *Redox Biol.* **2**, 123–139.
- Manevich, Y., Feinstein, S. I. and Fisher, A. B. (2004). Activation of the antioxidant enzyme 1-CYS peroxiredoxin requires glutathionylation mediated by heterodimerization with pi GST. *Proc. Natl. Acad. Sci. USA* **101**, 3780–3785.
- Martin, D. C., Kim, H., Mackin, N. A., Maldonado-Báez, L., Evangelista, C. C., Beaudry, V. G., Dudgeon, D. D., Naiman, D. Q., Erdman, S. E. and Cunningham, K. W. (2011). New regulators of a high affinity  $\text{Ca}^{2+}$  influx system revealed through a genome-wide screen in yeast. *J. Biol. Chem.* **286**, 10744–10754.
- Menon, D. and Board, P. G. (2013). A Role for Glutathione Transferase Omega 1 (GSTO1-1) in the Glutathionylation Cycle. *J. Biol. Chem.* **288**, 25769–25779.
- Muller, E. M., Locke, E. G. and Cunningham, K. W. (2001). Differential regulation of two  $\text{Ca}^{2+}$  influx systems by pheromone signaling in *Saccharomyces cerevisiae*. *Genetics* **159**, 1527–1538.
- Muralidharan, P., Cserne Szappanos, H., Ingley, E. and Hool, L. (2016). Evidence for redox sensing by a human cardiac calcium channel. *Sci. Rep.* **6**, 19067.
- Nakajima-Shimada, J., Iida, H., Tsuji, F. I. and Anraku, Y. (1991). Monitoring of intracellular calcium in *Saccharomyces cerevisiae* with an apoaequorin cDNA expression system. *Proc. Natl. Acad. Sci. USA* **88**, 6878–6882.
- Paidhungat, M. and Garrett, S. (1997). A homolog of mammalian, voltage-gated calcium channels mediates yeast pheromone-stimulated  $\text{Ca}^{2+}$  uptake and exacerbates the *cdc1(Ts)* growth defect. *Mol. Cell. Biol.* **17**, 6339–6347.
- Popa, C.-V., Dumitru, I., Ruta, L. L., Danet, A. F. and Farcasanu, I. C. (2010). Exogenous oxidative stress induces  $\text{Ca}^{2+}$  release in the yeast *Saccharomyces cerevisiae*. *FEBS J.* **277**, 4027–4038.
- Pozniakovsky, A. I., Knorre, D. A., Markova, O. V., Hyman, A. A., Skulachev, V. P. and Severin, F. F. (2005). Role of mitochondria in the pheromone- and amiodarone-induced programmed death of yeast. *J. Cell Biol.* **168**, 257–269.
- Puigpinós, J., Casas, C. and Herrero, E. (2015). Altered intracellular calcium homeostasis and endoplasmic reticulum redox state in *Saccharomyces cerevisiae* cells lacking Grx6 glutaredoxin. *Mol. Biol. Cell* **26**, 104–116.
- Rinnerthaler, M., Büttner, S., Laun, P., Heeren, G., Felder, T. K., Klinger, H., Weinberger, M., Stolze, K., Grousl, T., Hasek, J. et al. (2012). Yno1p/Aim14p, a NADPH-oxidase ortholog, controls extramitochondrial reactive oxygen species generation, apoptosis, and actin cable formation in yeast. *Proc. Natl. Acad. Sci. USA* **109**, 8658–8663.
- Tang, H., Viola, H. M., Filipovska, A. and Hool, L. C. (2011).  $\text{Ca}^{2+}$  1.2 calcium channel is glutathionylated during oxidative stress in guinea pig and ischemic human heart. *Free Radic. Biol. Med.* **51**, 1501–1511.
- Teng, J., Iida, K., Imai, A., Nakano, M., Tada, T. and Iida, H. (2013). Hyperactive and hypoactive mutations in Cch1, a yeast homologue of the voltage-gated calcium-channel pore-forming subunit. *Microbiology* **159**, 970–979.
- Todorovic, S. M. and Jevtovic-Todorovic, V. (2014). Redox regulation of neuronal voltage-gated calcium channels. *Antioxid. Redox Signal.* **21**, 880–891.
- Viladevall, L., Serrano, R., Ruiz, A., Domenech, G., Giraldo, J., Barceló, A. and Ariño, J. (2004). Characterization of the calcium-mediated response to alkaline stress in *Saccharomyces cerevisiae*. *J. Biol. Chem.* **279**, 43614–43624.
- Vu, K., Bautos, J., Hong, M.-P. and Gelli, A. (2009). The functional expression of toxic genes: Lessons learned from molecular cloning of CCH1, a high-affinity  $\text{Ca}^{2+}$  channel. *Anal. Biochem.* **393**, 234–241.
- Zhang, N.-N., Dudgeon, D. D., Paliwal, S., Levchenko, A., Grote, E. and Cunningham, K. W. (2006). Multiple signaling pathways regulate yeast cell death during the response to mating pheromones. *Mol. Biol. Cell* **17**, 3409–3422.